

Broadband, unpolarized repumping and clearout light sources for Sr^+ single-ion clocks

T. Fordell,^{1,*} T. Lindvall,¹ P. Dubé,² A.A. Madej,² A.E. Wallin,¹ and M. Merimaa¹

¹*VTT Technical Research Centre of Finland Ltd,*

Centre for Metrology MIKES, P.O.Box 1000, FI-02044 VTT, Finland

²*Frequency and Time Group, Measurement Science and Standards Portfolio,
National Research Council of Canada, Ottawa, Canada K1A 0R6*

Future transportable optical clocks require compact and reliable light sources. Here, broadband, unpolarized repumper and state clearout sources for Sr^+ single-ion optical clocks are reported. These turn-key devices require no frequency stabilization nor external modulators. They are fiber based, inexpensive, and compact. Key characteristics for clock operation are presented, including optical spectra, induced light shifts and required extinction ratios. Tests with an operating single-ion standard show a clearout efficiency of 100%. Compared to a laser-based repumper, the achievable fluorescence rates for ion detection are a few tens of per cent lower. The resulting ion kinetic temperature is 1–1.5 mK, near the Doppler limit of the ion system. Similar repumper light sources could be made for Ca^+ (866 nm) and Ba^+ (650 nm) using semiconductor gain media.

This paper was published in Optics Letters and is made available as an electronic reprint with the permission of OSA. The paper can be found at the following URL on the OSA website: <http://www.opticsinfobase.org/ol/abstract.cfm?uri=ol-40-8-1822>. Systematic or multiple reproduction or distribution to multiple locations via electronic or other means is prohibited and is subject to penalties under law.

The fractional uncertainties of several types of optical clocks are at or approaching the 10^{-18} level [1–5], which is equivalent to a change in the gravitational redshift caused by a height difference of only 1 cm. Since such detailed knowledge on the gravitational potential is currently not available, clock comparisons at the lowest uncertainty level must be done locally. Therefore, transportable optical clocks (TOCs) are needed. Besides time-keeping, TOCs will aid the search for variations in the fundamental constants [6], and their gravitational sensitivity could find interesting applications such as geodesy [7]. TOCs could also replace masers as local oscillators at remote radio telescopes and thereby improve resolution in very-long baseline interferometry.

Practical transportability calls for compactness and robustness on all parts of a clock. In addition to the extremely stable clock laser, an optical clock requires several other light sources that must address electronic transitions in the reference ion or atoms. Many optical frequency/time references require ‘repumper’ light sources to provide optical pumping out of undesired metastable levels. In addition, rapid resetting of the upper state of a clock transition via a ‘clearout’ light source is frequently required so that the optical reference can have low dead time and frequency instabilities approaching the quantum measurement limits of the system. If lasers are used, wavelength stabilization is required, which adds complexity and calls for continuous operation of the lasers. Frequency stabilization is not needed if broadband sources are used, as proposed and theoretically studied in [8] for the case of the repumper and clearout light sources

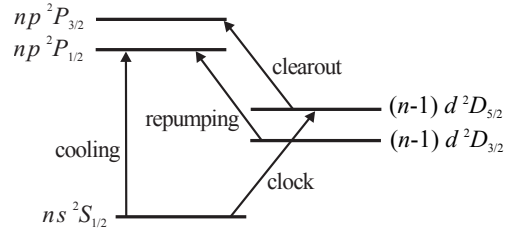


FIG. 1. Partial energy level diagram of Sr^+ ($n = 5$). Other clock ions with similar structure include Ca^+ ($n = 4$), and Ba^+ ($n = 6$).

needed in single-ion optical clocks. If the broadband repumper is also unpolarized, the formation of dark states [9] is prevented in a zero magnetic field without any external modulators [10, 11]. This article reports on the construction of such broadband, amplified spontaneous emission (ASE) sources for a Sr^+ single-ion optical clock. Key characteristics, including output spectra, achievable fluorescence rates, induced light shifts, modulation response and ion kinetic temperatures are discussed below.

The $^{88}\text{Sr}^+$ system (Fig. 1), whose reference or clock line is the dipole forbidden $5s\ ^2S_{1/2} \rightarrow 4d\ ^2D_{5/2}$ transition at 445 THz (674 nm), is one of the single ion systems being studied as a potential optical atomic clock. The ion is laser cooled on the 422-nm $5s\ ^2S_{1/2} \rightarrow 5p\ ^2P_{1/2}$ resonance line transition using a laser source. With a natural linewidth of 22 MHz, the ion kinetic temperature can reach a Doppler cooling limit of 0.5 mK. When probed on the 674 nm reference transition, interruption of the strong S-P fluorescence corresponds to probe excitation into the upper state of the clock transition and is thus used to sense the excitation with near unity de-

* Corresponding author: thomas.fordell@vtt.fi

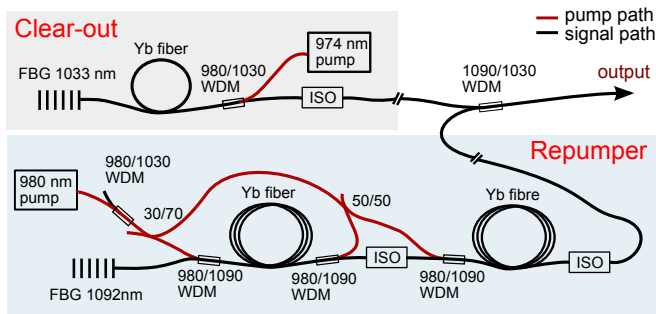


FIG. 2. Amplified spontaneous emission source layout. WDM: wavelength division multiplexer; FBG: fiber bragg grating; ISO: optical isolator.

tection efficiency. In addition to these two key laser-based sources, other light sources are necessary for the ion reference to operate effectively. Due to dipole-allowed relaxation from the $5p^2P_{1/2}$ level, a repumper is required on the $4d^2D_{3/2} \rightarrow 5p^2P_{1/2}$ transition at 1092 nm. Also, once the ion is excited into the long-lived $4d^2D_{5/2}$ level, a rapid means to return the ion from the upper state is necessary to reduce dead time in the laser cooling / probe / detection cycle. The method of choice is to use a state clearout source at 1033 nm to excite the $4d^2D_{5/2} \rightarrow 5p^2P_{3/2}$ transition whereupon rapid decay at the ns time scale returns the ion to the ground state.

The clearout and repumper are based on ASE in Yb-doped fibers. The layout is shown in Fig. 2. The main part of both sources is an Yb-doped fiber, the back end of which is spliced to a narrowband (1-nm) fiber Bragg grating (FBG) reflector. The other (output) end is left open. For the clearout radiation at 1033 nm, a backward pumped 80-cm Yb-doped fiber is used together with a two-stage, polarization insensitive isolator that prevents lasing due to optical feedback. The output spectrum is shown in Fig. 3 (solid red line) at an approximate maximum pump power of 80 mW.

The power requirement for the repumper is three orders of magnitude higher than for the clearout, and this, together with the reduced gain at the longer wavelength, complicates the design. In the first stage, the repumper uses a 10-m Yb-doped fiber that is pumped at both ends. To boost the output power and filter the spectrum, another 10-m Yb-doped fiber is used. With only forward pumping, this second fiber amplifies the signal at 1092 nm while at the same time attenuating heavily radiation at 1033 nm, which is important to avoid clearing out the clock state. The resulting output spectrum is shown in Fig. 3 (solid black) for a total pump power of roughly 650 mW.

To guide the design, a simple numerical two-level model [12] was developed that takes into account the gain medium, the FBGs, the WDMs and losses in the isolators. Without detailed information on the doping profile, a step-like profile was assumed, the width of which was adjusted so that the peak experimental and numerical

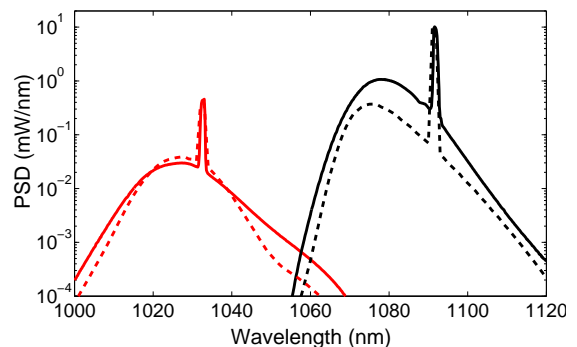


FIG. 3. Measured clearout (solid red) and repumper (solid black) output power spectral densities (PSD). Also shown are spectra based on a numerical model (dashed).

PSDs matched approximately. The output of this simple model for the repumper and clearout is shown by the black and red dashed curves, respectively. The higher-than-expected background in the repumper spectrum is probably caused by reflections from optical components unaccounted for in the model or from a shortcoming of the two-level model used.

The ASE device was tested and compared against 1092-nm and 1033-nm lasers used in the Sr^+ single-ion optical clock facility at the National Research Council of Canada [4, 13]. Briefly, a single atomic ion of $^{88}\text{Sr}^+$ is held in an electrodynamic trapping field using a miniature radio frequency endcap trap [13]. The ion trap is operated at a frequency of $\Omega = 2\pi \times 14.4$ MHz with a voltage amplitude of $V_o = 215$ V. A frequency stabilized, direct diode laser source at 422 nm is used as the primary laser cooling / fluorescence source. A diode-pumped fiber laser usually provides the repump for the $4d^2D_{3/2} \rightarrow 5p^2P_{1/2}$ transition at 1092 nm while state clearout is achieved with an external-cavity diode laser at 1033 nm. Both the 1092-nm and 1033-nm laser sources are frequency stabilized to a reference Fabry-Perot cavity whose absolute length is controlled by reference to a 633 nm polarization-stabilized HeNe laser. Detected fluorescence rates of 10^4 counts per second are observed with a signal to background ratio of better than 50. Interruption of this strong S-P fluorescence corresponds to probe excitation into the upper state of the clock transition. The probe system [14] consistently shows line resolutions down to 4 Hz. A removable mirror was used to rapidly switch between the laser and ASE light sources. By enlarging the ASE beams as much as possible before beam combination, beam waists at the ion of approximately $41 \mu\text{m}$ and $54 \mu\text{m}$ were obtained for the repumper and clearout, respectively, with 64% losses between source output and the ion.

For clock operation, the cooling light scattered by the ion must be sufficient for reliable state detection. The measured total ion fluorescence rates are shown in Fig. 4 as a function of the effective Rabi frequency squared (proportional to intensity) per bandwidth Θ [8]. The total ion

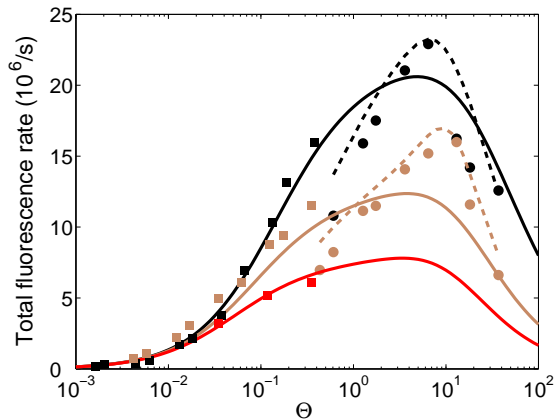


FIG. 4. Total fluorescence rates for the ASE and laser repumpers as a function of the effective Rabi frequency squared per bandwidth Θ . The solid circles represent data obtained with the laser repumper while the solid squares show data using the ASE repumper. Three cooling laser intensities were used: 550 W/m^2 (red), 1100 W/m^2 (brown) and 3300 W/m^2 (black), corresponding to the Rabi frequencies $\Omega_c/\Gamma = 1.2$, 1.7 , and 2.9 , respectively. Theoretical values are shown with solid (ASE) and dashed (laser) lines.

fluorescence rate was determined from that detected by carefully taking into account the detector response and losses in the imaging system (geometry and lens coatings). The power of a laser repumper is obtained from the relation $P_1 = 612.1 \text{ W/m}^2 \cdot w_1^{-2} \cdot \Theta_1$, where w_1 is the beam waist. For a laser $\Theta_1 = (\Omega_r/\Gamma)^2$, where Ω_r is the Rabi frequency and $\Gamma/2\pi = 21.6 \text{ MHz}$ is the natural linewidth of the $P_{1/2}$ excited state. For the broadband ASE repumper, the power spectral density (PSD) at resonance is given by $\Phi_{\text{ASE}} = 5.415 \text{ } \mu\text{W/nm} \cdot (w_{\text{ASE}}/\lambda)^2 \cdot \Theta_{\text{ASE}}$, where λ is the wavelength and $\Theta_{\text{ASE}} = \Omega_r^2/(b\Gamma)$, where b is the (Lorentzian) linewidth of the source. For the theoretical results shown in Fig. 4, the median of the intensities from light shift measurements reported in Fig. 6 was used to relate the power of the ASE source to the intensities. With no free parameters, the agreement between theory and experiment is quite good.

In order to minimize the second-order Doppler shift due to thermal motion and its uncertainty, the ion temperature must be characterized. Temperature was determined by measuring the ion thermal velocity using ratios of the secular sidebands to the carrier [13]. With resolved Zeeman sidebands ($B = 0.2 \text{ } \mu\text{T}$), the kinetic temperatures in the three canonical trap directions are shown in Fig. 5 for the laser and ASE repumpers (red and black circles, respectively). The cooling laser intensity was 1700 W/m^2 . For the ASE repumper, the temperature was also determined using a collapsed Zeeman spectrum (low B-field), the result of which (black triangles) was in very good agreement with the previous result. By lowering the cooling intensity to 930 W/m^2 , a reduction in temperature could be observed (black squares). While both sources enable cooling close to the Doppler

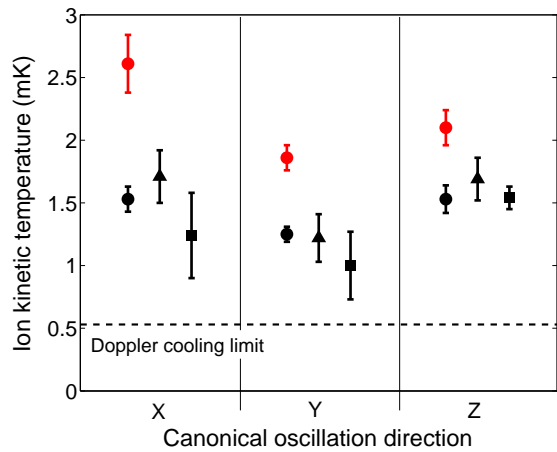


FIG. 5. Measured ion kinetic temperatures using Zeeman-resolved motional sidebands with a laser repumper (red circles) and the ASE repumper (black circles). The 422 nm laser cooling intensity was 1700 W/m^2 . Temperature measurements with a collapsed Zeeman spectrum (low B field) gave similar results (ASE source only, black triangles). Also shown is the measured temperature when the cooling intensity was lowered to 930 W/m^2 (ASE source only, black squares). The errorbars equal one standard deviation. The Z-axis is the symmetry axis of the endcap trap.

limit, the ASE repumper seems to yield somewhat lower temperatures.

Due to the broad linewidths, the power needed for efficient repumping and clearout is about four orders of magnitude larger for the ASE sources than for lasers; therefore, the light shifts must be measured so that sufficient extinction can be applied during the probe pulse. Fig. 6 shows three measurements of the light shift caused by the ASE repumper. Like the electric quadrupole shift [15], the light shift depends linearly on m_j^2 of the $4d^2D_{5/2}$ clock state. The data is well aligned with the theoretical predictions for a completely unpolarized repumper (solid lines). The light shifts were calculated by summing the contributions from all transitions listed in [16] (tables 1–2), taking into account the fractions of π and σ polarization. The spectrum of the ASE source (Fig. 3) was accounted for by expressing it as a sum of Lorentzian lines with the same total area, and adding the light shifts caused by the individual Lorentzians. The only free parameter is the intensity, and a fit to the data yields 2.49 MW/m^2 , 2.87 MW/m^2 , and 3.15 MW/m^2 . These values agree with the experimental estimate of 3.9 MW/m^2 for a perfectly aligned beam with a 1.0 Strehl ratio. Also shown is the expected behavior for π - (dotted) and σ -polarized light (dashed). The difference in slopes between the experiment and theory is probably due to the light not being perfectly unpolarized.

Light shifts caused by the clearout source were investigated by running it continuously at power levels where the clearout efficiency was very low. Extrapolating the data for the $m_J = -\frac{1}{2} \rightarrow \frac{1}{2}$ Zeeman component to 'work-

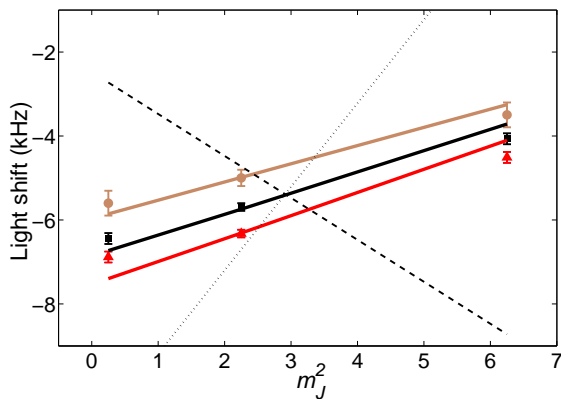


FIG. 6. Measured light shifts of the Zeeman components caused by the ASE repumper as a function of m_J^2 of the upper state of the clock transition. Solid lines show theoretical predictions for an unpolarized ASE light source with the intensities 2.49 MW/m² (brown), 2.87 MW/m² (black), and 3.15 MW/m² (red). Also shown is the expected behavior for π -polarized (dotted) and σ -polarized light (dashed).

ing conditions' points towards 10 Hz order of magnitude light shifts if the source is on continuously.

A very convenient feature of the ASE light sources is that they can be electronically turned on and off during the clock cycle by modulating the pump diodes. The important parameters are then the turn-on and turn-off times and, especially, the extinction ratio. The turn-on time is about 4 ms (0-90%). At turn off, stimulated emission dominates and the power drops quickly by two orders of magnitude. After that, the light decay reflects the upper state lifetime ($\approx 900 \mu\text{s}$). If the average fractional light shift of the clock transition during a 100 ms probe pulse is required to be at the 10^{-19} level, then, due to the exponential decay of the ASE sources, the shift should

be at the 10^{-17} level at the beginning of the probe pulse. The measured light shifts translate into an extinction ratio requirement at the start of the clock pulse of $\gtrsim 10^6$ for the repumper and $\gtrsim 10^4$ for the clearout. Measured values indicate that the repumper and clearout will decay to this level after the current is turned off in approximately 8 ms and 4 ms, respectively.

Clearout efficiency was tested with 5 ms pulses by varying the output power of the ASE source. The efficiency was 100% at medium to high output powers. A drop to about 90% at an estimated $170 \frac{\text{W}}{\text{nm}^2}$ (or 2300 W/m^2) was observed, corresponding to a light source output of only $2.2 \mu\text{W/nm}$. Independent calculations showed that at an intensity level of $160 \frac{\text{W}}{\text{nm}^2}$, the probability of the electron remaining in the D-state has risen to approximately 10%, in good agreement with what was experimentally observed.

In conclusion, key characteristics of the ASE light sources have been presented and their suitability for use in state-of-the-art optical single-ion clocks has been verified. Still lower light shifts can be obtained using more narrowband FBGs and/or external narrowband interference filters. The numerical model can be used to further optimize the design, and if higher PSDs are needed additional gain stages can be easily added. Similar repumpers could be made for Ca^+ (866 nm) and Ba^+ (650 nm) using semiconductor gain media.

This work was supported by the Academy of Finland (project 138894) and by the European Metrology Research Program (EMRP) in project SIB04. The EMRP is jointly funded by the EMRP participating countries within EURAMET and the European Union. TF acknowledges financial support from the European Commission (Marie Curie Integration Grant PCIG10-GA-2011-304084).

-
- [1] C. W. Chou, D. B. Hume, J. C. J. Koelemeij, D. J. Wineland, and T. Rosenband, *Phys. Rev. Lett.* **104**, 070802 (2010).
- [2] N. Hinkley, J. A. Sherman, N. B. Phillips, M. Schioppo, N. D. Lemke, K. Bely, M. Pizzocaro, C. W. Oates, and A. D. Ludlow, *Science* **341**, 1215 (2013).
- [3] B. J. Bloom, T. L. Nicholson, J. R. Williams, S. L. Campbell, M. Bishof, X. Zhang, W. Zhang, S. L. Bromley, and J. Ye, *Nature* **506**, 71 (2014).
- [4] P. Dubé, A. A. Madej, M. Tibbo, and J. E. Bernard, *Phys. Rev. Lett.* **112**, 173002 (2014).
- [5] G. P. Barwood, G. Huang, H. A. Klein, L. A. M. Johnson, S. A. King, H. S. Margolis, K. Szymaniec, and P. Gill, *Phys. Rev. A* **89**, 050501 (2014).
- [6] R. M. Godun, P. B. R. Nisbet-Jones, J. M. Jones, S. A. King, L. A. M. Johnson, H. S. Margolis, K. Szymaniec, S. N. Lea, K. Bongs, and P. Gill, *Phys. Rev. Lett.* **113**, 210801 (2014).
- [7] C. W. Chou, D. B. Hume, T. Rosenband, and D. J. Wineland, *Science* **329**, 1630 (2010).
- [8] T. Lindvall, T. Fordell, I. Tittonen, and M. Merimaa, *Phys. Rev. A* **87**, 013439 (2013).
- [9] T. Lindvall, M. Merimaa, I. Tittonen, and A. A. Madej, *Phys. Rev. A* **86**, 033403 (2012).
- [10] G. P. Barwood, P. Gill, G. Huang, H. A. Klein, and W. R. C. Rowley, *Opt. Commun.* **151**, 50 (1998).
- [11] D. J. Berkeland, J. D. Miller, J. C. Bergquist, W. M. Itano, and D. J. Wineland, *Phys. Rev. Lett.* **80**, 2089 (1998).
- [12] E. Desurvire, *Erbium-doped fiber amplifiers* (John Wiley & Sons, Inc., 2002) pp. 28–31.
- [13] P. Dubé, A. A. Madej, Z. Zhou, and J. E. Bernard, *Phys. Rev. A* **87**, 023806 (2013).
- [14] P. Dubé, A. A. Madej, J. E. Bernard, L. Marmet, and A. D. Shiner, *Appl. Phys. B* **95**, 43 (2009).
- [15] P. Dubé, A. A. Madej, J. E. Bernard, L. Marmet, J.-S. Boulanger, and S. Cundy, *Phys. Rev. Lett.* **95**, 033001 (2005).
- [16] D. Jiang, B. Arora, M. S. Safronova, and C. W. Clark, *J. Phys. B: At. Mol. Opt. Phys.* **42**, 154020 (2009).